

## In-flight determination of the AMS-RICH photon yield

F. GIOVACCHINI<sup>1</sup>, I. RODRÍGUEZ<sup>1</sup> ON BEHALF OF THE AMS02-RICH COLLABORATION.

<sup>1</sup> *Centro de Investigaciones Energéticas, Medioambientales y Tecnológicas (CIEMAT, Madrid, Spain)*

*francesca.giovacchini@cern.ch*

**Abstract:** AMS-02 was installed on the International Space Station (ISS) in May 2011 to perform precise measurements of Galactic cosmic rays in the 100 MV to few TV magnetic rigidity range by means of specialized sub-detectors. The Ring Imaging Cherenkov (RICH) provides AMS with a precise measurement of the particle velocity and charge. The RICH radiator is composed of a layer of silica aerogel and sodium fluoride. The Cherenkov light is detected by means of an array of photomultiplier tubes. Optimal performance of the detector requires the knowledge of the effective photon yield at the percent level. Temperature corrections to the photodetectors response are determined using in-flight data. The residual photon yield variation after corrections is well within the requirements. The remaining uncertainties on the photon yield are accounted as effective non-uniformities in the radiator and are estimated using in-flight data. After 2 years of operation on the ISS, more than 95% of the detection channels are in nominal operation conditions and no degradation is observed on the effective photon yield. Charge resolution is 0.3 charge units for Z=2, 0.5 charge units for Z=14. This is consistent with a remaining uncertainty on the photon yield better than 3%.

**Keywords:** Cosmic-Rays, Cherenkov Radiation, RICH, AMS, Detection Techniques

## Introduction

AMS-02, the Alpha Magnetic Spectrometer, is a high energy particle detector that operates on the International Space Station (ISS). AMS was installed on May 16<sup>th</sup> 2011 and started science data acquisition on May 19<sup>th</sup> 2011. Since then, it has operated continuously and collected over  $3 \times 10^{10}$  events.

The measurement principle of a magnetic spectrometer relies on the deviation that charged particle trajectories suffer when crossing the magnetic field. In AMS, a cylindrical permanent magnet generates a uniform field in its bore. The Silicon Tracker Detector (STD) provides a very accurate value of the curvature thus providing particle momentum and charge sign. Velocity is determined by the Time of Flight system (TOF) and by the RICH. Finally, the absolute value of the charge is independently measured by the Transition Radiation Detector (TRD), TOF, STD and RICH. Particle identification is reinforced with the TRD and the Electromagnetic Calorimeter (ECAL), which are able to distinguish between protons and electrons.

The precise determinations of the particle velocity and charge provided by the RICH require detailed knowledge and careful monitoring of all detector parameters. Calibration methods using in-flight data have been developed to optimize the detector performance in space for both velocity and charge reconstruction. Velocity calibration and monitoring is treated in a separate contribution [1]. Here, the methods applied to the charge reconstruction are presented and the results are summarized. The RICH detector is described in Sec. 1 and the algorithm for charge measurement is introduced in Sec. 2. The calibration procedures for time dependent and time independent corrections are described in Secs. 3 and 4. Finally, the impact of these corrections on the detector performance are shown on in Sec. 5.

## 1 The RICH detector

The AMS Ring Imaging Cherenkov counter (RICH) is designed to provide precise measurements of the velocity and absolute charge of relativistic particles [2]- [9]. The RICH consists of a layer of radiator material, a conical reflector and a detection plane (see Fig. 1). When a charged particle crosses the radiator at a velocity greater than the Cherenkov threshold a cone of light is emitted. The Cherenkov radiation propagates through an expansion volume to the detection plane, where an array of photodetectors measures its footprint. The conical reflector defines the expansion volume and redirects to the detection plane the radiation which otherwise would escape its acceptance.

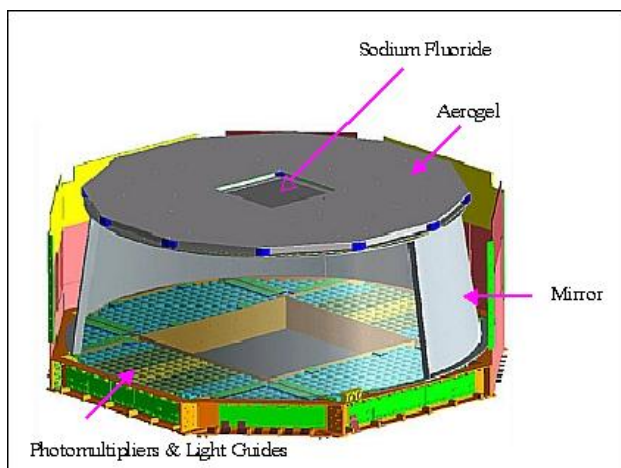


**Figure 1:** Schematic view of the AMS-02 RICH. The different parts of the detector are indicated in the figure.

In AMS, most events consist in a single particle crossing the radiator. The particle velocity,  $\beta$ , is measured by esti-

mating the Cherenkov cone half-angle,  $\theta_c$ , using the equation

$$\beta = \frac{1}{n \cdot \cos \theta_c} \quad (1)$$

where  $n$  is the radiator refractive index and determines the threshold for the measurement.

The absolute value of the particle electric charge,  $Z$ , is estimated from the intensity of the signal in the Cherenkov ring as the number of detected photoelectrons,  $N_{pe}$ , is proportional to  $Z^2$

$$N_{pe} \sim Z^2 \cdot \sin^2 \theta_c \quad (2)$$

The number of photoelectrons on each detection channel is derived from the detected signal relative to the average single photoelectron response, known as gain.

The RICH radiator consists of a set of 92 2.5 cm thick silica aerogel tiles (AGL) with a refractive index  $n = 1.05$  and 16 0.5 cm thick sodium fluoride crystals (NAF) with a refractive index of  $n = 1.33$  which cover the 120 cm diameter circle at the top of the reflector. AGL, which represents 90% of the radiator geometrical acceptance, provides the measurement of particles with  $\beta > 0.95$ , whereas NAF, covering the  $34 \times 34 \text{ cm}^2$  central square, is able to measure particles with  $\beta > 0.75$ .

The reflector consists of a highly reflective multilayer structure deposited on a carbon fiber substrate with a shape of a truncated cone with an upper diameter of 120 cm, 47 cm high and a bottom diameter of 124 cm. The detection plane is made of a set of 680 4x4 multianode photomultiplier tubes PM (Hamamatsu 7600-00-M16) with individual light guides to increase the effective area. The total number of readout channels is 10880 with a spatial granularity of  $8.5 \times 8.5 \text{ cm}^2$ . The RICH front-end electronics is mounted at the back of each PM. Anode pulses are shaped with a double gain 16-channel preamplifier and analog signals are digitized by means of a 12-bit ADC. The RICH readout and configuration is controlled by 24 data reduction modules. The dynamic range of the electronics extends from 1 to 100 photoelectrons with a single photoelectron resolution of about 50%. This ensures that the RICH is able to measure the velocity and charge of relativistic particles for  $Z \lesssim 26$  with resolutions  $\Delta\beta/\beta \lesssim 1\%$  and  $\Delta Z \lesssim 0.5$ .

The design performances of the RICH can only be achieved in the long term if the detector components show no significant degradation in space and the effects of the changing environmental conditions on the ISS can be correctly accounted.

Temperature variation and its gradient across the detector plane generate the most important time dependent effects to be monitored and corrected. The bias induced on the measured velocity is negligible being of the order of  $10^{-5}$  [1]. The effect on the photodetection system is twofold: first, it modifies the single photoelectron response, and second it affects the photodetection efficiency. Temperature constants, in the range of few parts per mil per degree, were first determined on ground on a subset of the photomultiplier tubes and have been reevaluated on flight data. A detailed map of the temperature of the detection plane is obtained by means of 96 temperature sensors, which are in thermal contact with the photodetectors, and are read out at least once per minute.

After 2 years in space, more than 95% of the readout channels are in nominal operation conditions. Moreover, the downtime generated by single event upsets on the electronics which require reloading the configuration or calibration tables is negligible for the detector operation.

## 2 Charge estimation algorithm

The measurement of the particle charge in the RICH relies on the measurement of the number of photoelectrons collected along the Cherenkov ring,  $N_{pe}$ , relative to the expected value for a singly charged particle with the same velocity and track parameters,  $N_{exp}$ , so that

$$Q^2 = \frac{N_{pe}}{N_{exp}} \quad (3)$$

where  $Q^2$  is the estimated particle charge squared.  $N_{pe}$  is obtained directly from the sum of the signals of individual photodetection channels relative to their gain.  $N_{exp}$  is a more involved quantity which needs to be computed on an event-by-event basis by means of a numerical integration which accounts for the Cherenkov production in the radiator, the losses along the path to detection plane and the detection efficiency of the photodetector system. The main parameters affecting  $N_{exp}$  are the detector geometry, the optical parameters of the radiator, the reflectivity of the conical reflector, the light guide efficiency and the quantum efficiency of individual photomultiplier tubes.

Extensive laboratory measurements were carried out prior to the final detector assembly to provide detailed information of these quantities for all detector components [2]. These measurements, as well as additional data on off-nominal channels, are included in the charge estimation.

There are two different types of effects that may induce a bias on the electric charge estimation in the RICH and need to be treated separately. On the one hand, detector response may change with time, on the other hand, the reference data for some detector part may not have been determined to the required precision. Both effects are corrected sequentially using time dependent and time independent corrections.

## 3 Charge time dependent corrections

Temperature is expected to be the most important time dependent environmental factor affecting the charge determination due to its effect on the photodetector system. Precise determination of the temperature constants for gain and efficiency on a channel-by-channel basis can only be achieved on a large statistics sample of flight data collected on a wide temperature range.

In the RICH, these corrections are computed using signals associated to Cherenkov rings reconstructed on high rigidity proton and helium events identified with the AMS tracker. The temperature dependence of the photoelectron detection efficiency for individual channels is computed on helium events from the ratio of used to expected signals at different temperatures, whereas for gains are estimated from the median of the signal spectrum collected on proton events at different temperatures.

The wide temperature excursion experienced by the photodetectors, above  $30^\circ\text{C}$  for all channels, provides the lever arm for a precise determination of the temperature coefficients for all channels. On the other hand, temperature gra-

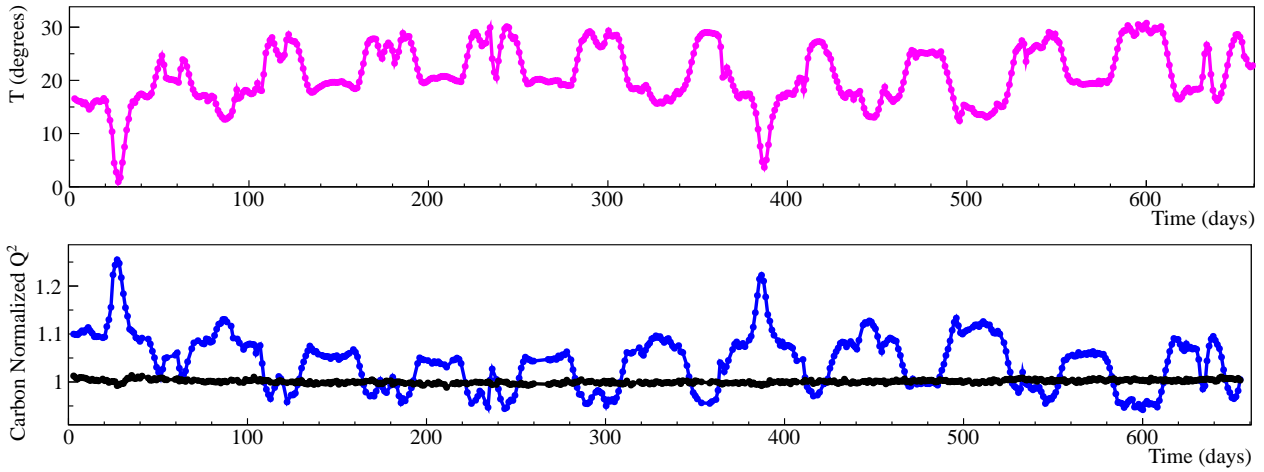


**Figure 2:** Evolution of the RICH detection plane average temperature throughout 660 days of operation (top) and of the deviation of the mean Cherenkov relative signal for Carbon,  $\frac{Q^2}{(Z=6)^2}$ , before (blue) and after (black) temperature corrections (bottom).

dients across the detector reaching 10°C require the detailed mapping obtained from the network of temperature sensors on the detection plane. Finally, the readout frequency of the temperature sensors is high enough to follow its evolution, since the maximum variation rate of the temperature at any location on the plane is below 1°C per hour. The evolution of the average temperature throughout 660 days of operation is shown in Fig. 2(top).

The temperature dependence of the photomultiplier response is linear within the studied range. The gain temperature coefficient is  $C_g = (-0.81 \pm 0.12(\text{RMS})) \text{ \%}/\text{^\circ C}$  and the efficiency temperature coefficient is  $C_e = (-0.23 \pm 0.14(\text{RMS})) \text{ \%}/\text{^\circ C}$ . The dispersion of these values justifies the need of using individual temperature coefficients for each single channel.

The relative deviation of the mean  $Q^2$  determined on Carbon samples recorded in periods of about 1 day is shown in Fig. 2(bottom). The clear correlation of these values and the average temperature shown in the top panel is removed after temperature corrections are applied.

The stability of the detector response after temperature corrections is well within 1% and does not compromise the accuracy of the charge determination. In addition, limits on possible long term degradation of the effective photon yield can be derived and show that, at the 95% confidence level, the photon yield variation is less than  $3 \times 10^{-6}/\text{day}$ , that is below 2% throughout the studied period.

#### 4 Charge time independent corrections

Once the fluctuations due to time dependent effects, as described in the previous section, are accounted, the computation of time independent corrections, so called uniformity corrections, should be addressed.

In spite of the knowledge of the detector coming from the determinations done on ground either during its construction or from measurements with cosmic muons, the required precision can only be achieved using high statistics samples of in-flight data.

Due to the interplay of the different potential effects affecting the ultimate precision on the measurement, an effective set of corrections is built using a subset of helium

events identified with the STD. The calibration sample is classified in a 5-dimensional phase space defined by:

- impact point at the radiator ( $X, Y$ )
- particle direction ( $\theta, \phi$ )
- particle reconstructed velocity ( $\beta$ )

For each 5-D bin, a correction factor is computed such that the average reconstructed charge corresponds to helium. This correction factor will be then applied to all events lying on this phase space bin. The phase space is divided in 30000 bins of 256 events each one.

The correction factors have a spread of 2%.

A projection map of the uniformity corrections as a function of the particle impact point on the radiator  $X$  and  $Y$  is shown in figure 3.

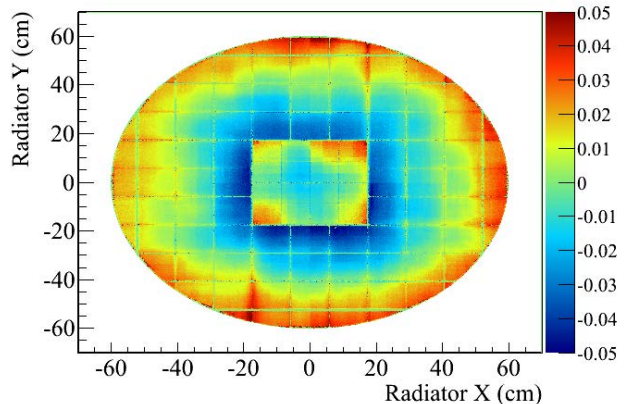


**Figure 3:** Map of the RICH uniformity corrections as a function of the particle impact point  $X$  and  $Y$  on the radiator plane.

## 5 Charge resolution

The impact of the corrections on the effective photon yield evaluation can be quantified as their effect on the resolution of the RICH charge measurement. The continuous charge estimator,  $\sqrt{Q^2}$ , is computed on samples of well identified ions selected with the STD and TOF from the first 2 years of flight data. For each ion sample, the charge resolution is defined as the width of a Gaussian distribution fitting the continuous charge estimator. The distribution for the selected helium sample is shown in Fig. 4.

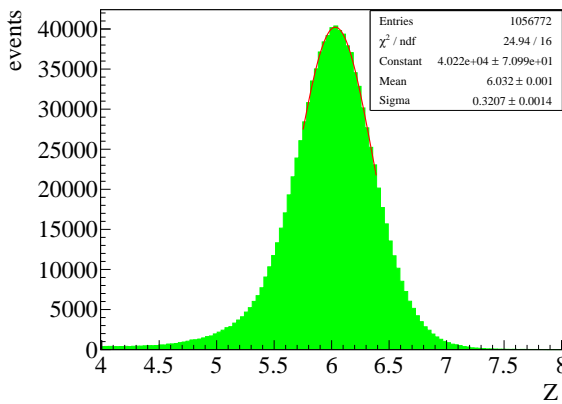


**Figure 4:** Reconstructed RICH charge distribution for selected helium sample is displayed together with the result of a fit of the peak region to a Gaussian distribution.

The evaluation of the RICH charge resolution on each sample is performed at different stages of the correction sequence: before corrections, after time dependent corrections and after all corrections are applied. The results for all selected ions at the different correction stages are shown in Fig. 5, where the improvement is clearly visible.

In order to quantify the remaining uncertainty on the photon yield computation on an event-by-event basis, it is convenient to parametrize the observed resolution on the absolute particle charge,  $Z$ , as the result of two effects added in quadrature

$$\sigma(Z) = 1/2 \sqrt{\sigma_{\text{stat}}^2 + Z^2 \sigma_{\text{sys}}^2} \quad (4)$$

where statistical uncertainties,  $\sigma_{\text{stat}}$ , arising from the finite number of photoelectrons available, define the optimal charge resolution achievable at any charge, whereas systematic uncertainties on the photon yield,  $\sigma_{\text{sys}}$ , reflecting the limited knowledge of the overall system response, scale linearly with the particle charge and constitute the leading contribution for high charges.

From fits to the observed evolution of the RICH charge resolution with  $Z$ , we conclude that the mean statistical contribution to the RICH charge resolution is 0.3 charge units. The systematic contributions before corrections are 5%, after time dependent corrections they are reduced to 4% and, after all corrections are applied, a residual 2.8% constitutes the current limit on the knowledge of the effective light yield.

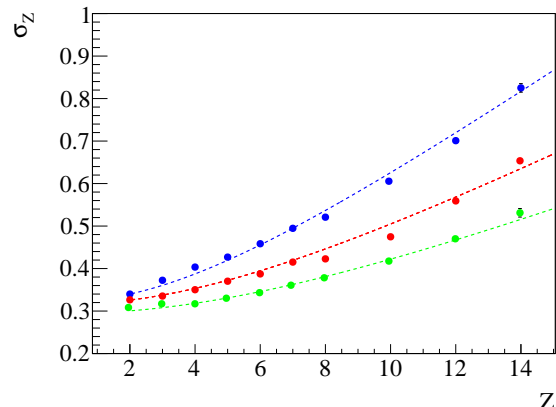


**Figure 5:** RICH Charge resolution for particles with charge from  $Z=2$  to  $Z=14$  for event crossing AGL radiator: in blue before corrections; in red after  $t$ -dependent corrections and in green after all corrections. Fits with eq. 4) are also shown.

## Conclusions

RICH detector system is adequately steady to determine the number of expected photoelectrons for each event, in order to infer its absolute electric charge. Remaining time residuals of aerogel charge final estimation, after calibrations and temperature dependent effects corrections, are well within requirements (less than 1%) which means no impact in charge resolution. Time stability of the measurement evinces no aging of silica aerogel during almost 2 years of operation. After performing the so called non uniformity corrections, RICH is able to distinguish different nuclei of cosmic rays up to Fe particles, providing charge measurements with resolutions better than 0.5 for light elements.

**Acknowledgment:** We acknowledge support from CIEMAT, CDTI, SEIDI-MINECO and CPAN, Spain; CNRS, IN2P3, CNES, Enigmass and ANR, France; Portuguese Foundation for Science and Technology.

## References

- [1] W.Gillard, proceedings to this conference n.742 .
- [2] M. Aguilar-Benitez et al., Nuclear Instruments and Methods in Physics Research A, **614**:237-249 (2010).
- [3] L. Sallaz-Damaz et al., Nuclear Instruments and Methods in Physics Research A **614**:184-195 (2010).
- [4] M. Aguilar-Benitez et al., Proc. 30th ICRC (2007), UNAM, Mexico City, **Vol. 2**:461-464 (2008).
- [5] L. Arruda et al., Nuclear Physics B Proceedings Supplements **172**:32-35 (2007).
- [6] P. Aguayo et al., Nuclear Instruments and Methods in Physics Research A **560**:291-302 (2006).
- [7] B. Baret et al., Nuclear Instruments and Methods in Physics Research A **525**:126 (2004).
- [8] D. Casadei, Nuclear Physics B Proceedings Supplements, **125**:303-307 (2003).
- [9] J. Casaus, Nucl Phys. B (Proc. Suppl.) **113**:147-153 (2002).